

6. RESULTS

This section discusses the measured characteristics of the various UWB interference sources, explains measured GPS operational and observational parameters, and summarizes trends.

6.1 UWB Spectral and Temporal Characteristics

In order to better understand the interference effects of UWB signals, it is helpful to understand their frequency and time-domain characteristics. A general description of the spectral features was given in Section 4.1.2. In this section, time-domain characteristics of the interfering signals are discussed.

When a narrow pulse, with a wide bandwidth (BW), is passed through a filter with a narrower bandwidth, the output is essentially equal to the impulse response of the filter and has a pulse width approximately equal to the reciprocal of the receiver bandwidth. Figure 6.1.1 illustrates 50%-ARD UWB signals, at three different PRFs, passed through a 20-MHz bandpass filter (center frequency of 1575.42 MHz) and downconverted to a center frequency of 321.4 MHz. The result is that, as the pulse passes through the filter, it becomes wider, the peak-to-average power decreases, and depending upon the PRF and extent of dithering, the pulses may overlap.

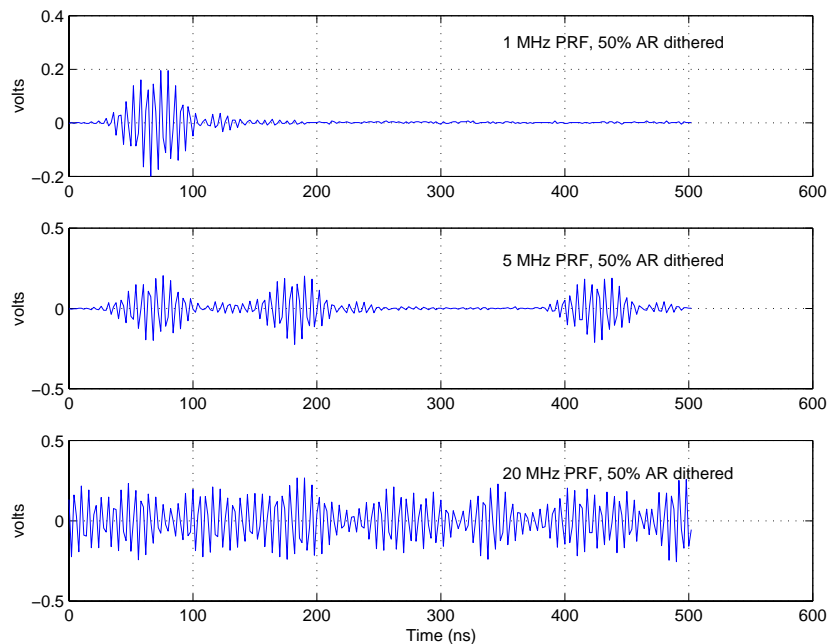


Figure 6.1.1. Temporal plots of 50%-ARD UWB signals passed through a 20-MHz bandpass filter and downconverted to a center frequency of 321.4 MHz.

One way to describe the time-domain characteristics is through APDs. These distributions are helpful for several reasons: when normalized to mean power, they can quickly show the relationship between peak, mean, and median power levels (as well as other percentiles); they reflect impulsiveness of the signal and the extent to which the signal power is present; they indicate the degree to which a signal is Gaussian; and they quickly distinguish signals that are constant amplitude in nature. APDs are particularly valuable, therefore, for providing statistical descriptions of wide bandwidth signals as they pass through the varying bandwidths of receivers. A tutorial on APDs is provided in Appendix E for those readers unfamiliar with their use.

A complete set of APDs, for each of the UWB signals used in these measurements, is provided in Appendix B. Additionally, a few composite APD plots are shown here for the purpose of illustration. For each of the composite plots, the mean power is normalized to 0 dBm so that the peak-to-average power can be readily determined. As a reference, an equivalent 0-dBm mean-power APD for Gaussian noise is plotted along with the UWB signals.

Figure 6.1.2 shows the normalized APDs for 8 different permutations of a UWB signal with a 100-kHz PRF. One can see that the amplitude distributions of the dithered signals are identical to the non-dithered cases. This is because, even for 50% ARD, the space between pulses is no less than 5 μ s apart; since the UWB pulse width after passing through a 3-MHz filter is approximately 300 ns, the pulses remain discrete and never overlap.

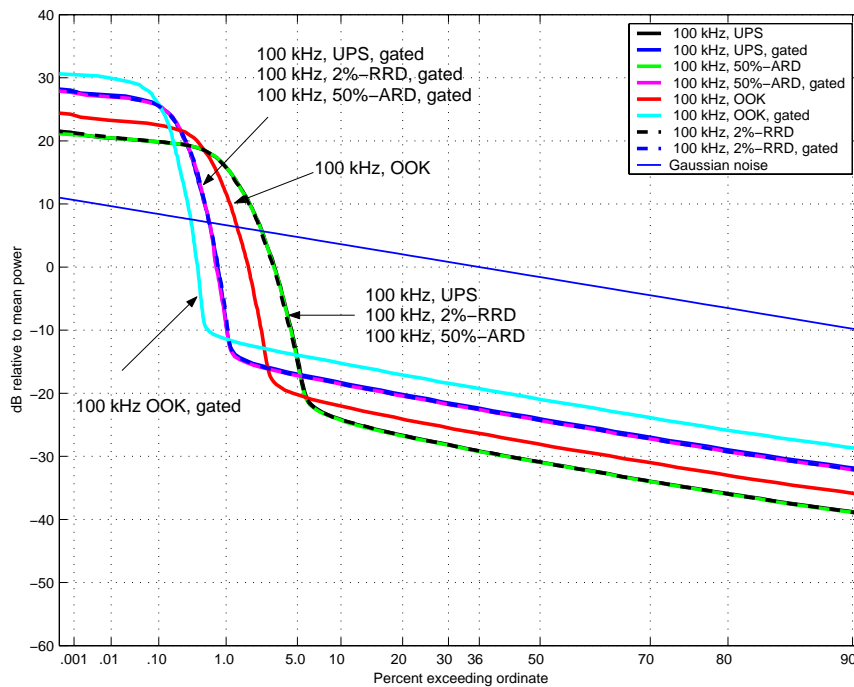


Figure 6.1.2. APDs of 100-kHz-PRF UWB signals measured in a 3-MHz bandwidth.

Therefore, while these dithered cases show a noise-like spectrum, they are non-Gaussian and impulsive with regard to their amplitude distributions.

Figure 6.1.3 shows the same plots for UWB signals with a PRF of 20 MHz. In this case, the UPS signal is sinusoidal (flat line), as we would expect since only one spectral line is allowed to pass through the 3-MHz filter. The dithered, non-gated cases, however, are Gaussian distributed. This is because the 20-MHz PRF is high enough to cause pulse overlap. Therefore, any random variations in the pulse spacing results in destructive and constructive addition of adjacent pulses and an apparent Gaussian distribution.

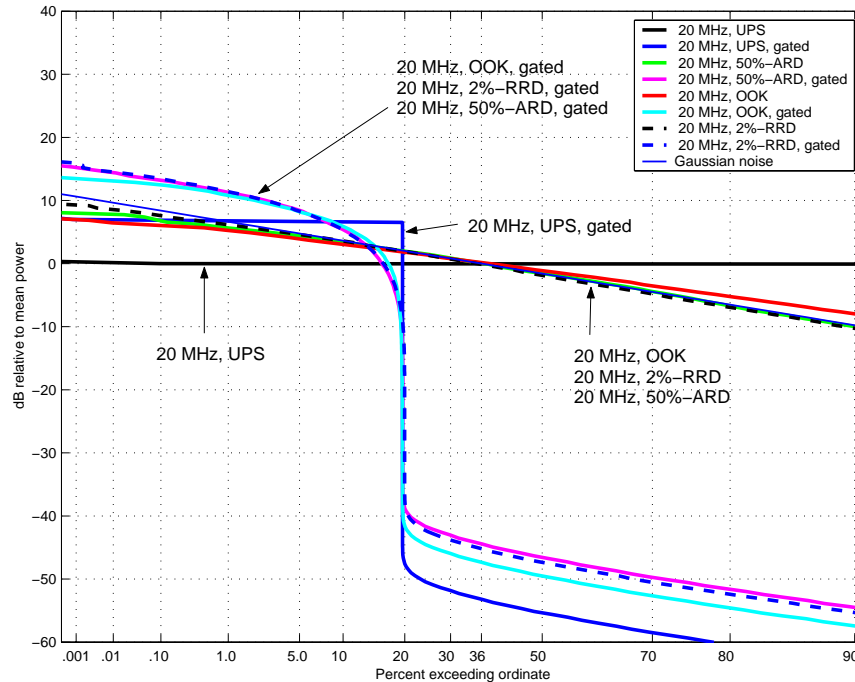


Figure 6.1.3. APDs of 20-MHz-PRF UWB signals measured in a 3-MHz bandwidth.

Figure 6.1.4 shows variations in amplitude distributions for 50% ARD pulses, varied with regard to PRF and passed through a 3-MHz bandwidth filter. One can see a natural progression as the pulses become more closely spaced: the pulse energy is present a greater percentage of the time, and as the pulses start to overlap, the signal amplitude distribution becomes more Gaussian-like.

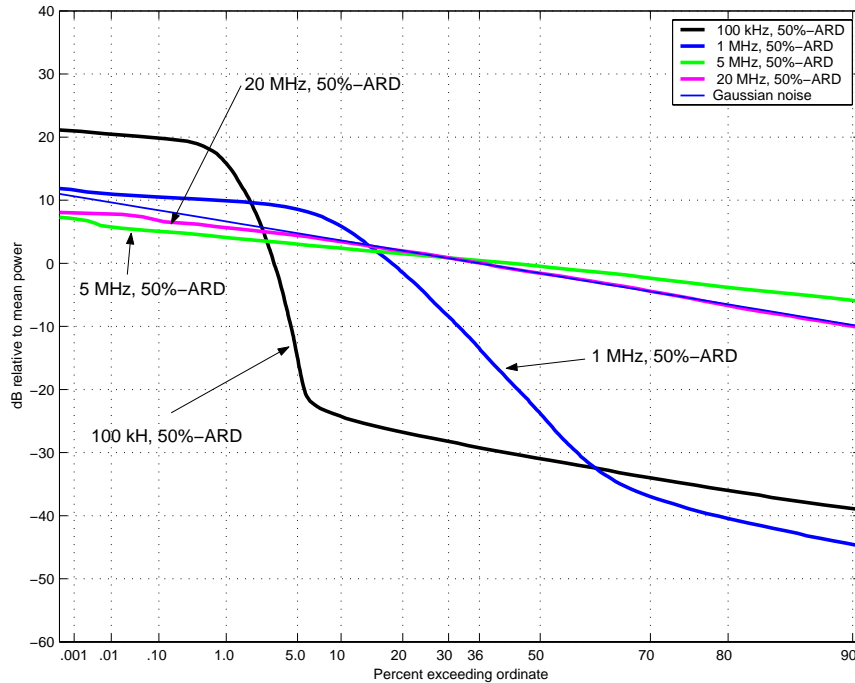


Figure 6.1.4. APDs of 50%-ARD UWB signals measured in a 3-MHz bandwidth.

6.2 GPS Interference Measurement Results

As discussed in the data analysis section, certain operational and observational metrics were chosen to demonstrate GPS receiver performance degradation. Results are given to establish how receivers respond to increasing levels of Gaussian noise with no UWB interference. Composite single-source and aggregate UWB results are provided to relate trends in GPS performance degradation to UWB interference parameters (e.g., PRF, pulse spacing). Whenever relevant, gated UWB results are plotted directly below non-gated UWB results to demonstrate the effects of gating. Table 6.2.1 gives a summary of the Figures under discussion in this section.

Table 6.2.1. Composite Figure List

| Interference | Rx 1 | | | Rx 2 | | |
|--------------|------------------|----------|---------|------------------|----------|-----|
| | BL | RQT | CMC | BL | RQT | CMC |
| Noise | 6.2.1.1, 6.2.1.2 | 6.2.1.8 | 6.2.2.1 | 6.2.1.3, 6.2.1.4 | 6.2.1.8 | N/A |
| UPS | 6.2.1.1, 6.2.1.2 | N/A | 6.2.2.2 | 6.2.1.3, 6.2.1.4 | N/A | N/A |
| OOK | 6.2.1.1, 6.2.1.2 | N/A | 6.2.2.3 | 6.2.1.3, 6.2.1.4 | N/A | N/A |
| 2%-RRD | 6.2.1.1, 6.2.1.2 | 6.2.1.9 | 6.2.2.4 | 6.2.1.3, 6.2.1.4 | 6.2.1.11 | N/A |
| 50%-ARD | 6.2.1.1, 6.2.1.2 | 6.2.1.10 | 6.2.2.5 | 6.2.1.3, 6.2.1.4 | 6.2.1.12 | N/A |
| Aggregate | 6.2.1.7 | 6.2.1.13 | 6.2.2.6 | N/A | N/A | N/A |

Figures 6.2.1 through 6.2.5 are composite graphs showing the BL point for each of the UWB permutations. For those cases where no BL point is displayed, the receiver never lost lock. RQT results are given in Figures 6.2.6 through 6.2.11. CMC residual-error standard deviation was chosen to demonstrate UWB interference effects and is plotted in Figures 6.2.12 through 6.2.16.

In addition, Appendix F provides a comprehensive set of plots – each set summarizing results for type of UWB interference to a specific receiver. The plots on the left side pertain to the code-tracking loop and display CMC statistics (recall that CMC statistics are dominated by PSR statistics). Error-residual percentiles and standard deviation are shown on the upper left, and measures to quantify skewness, excess, and independence are given on the lower left. The upper-right plots provide information pertaining to carrier-loop tracking such as ADR percentiles and cycle slip conditions. Often, cycle slip conditions correlate to SNR estimated by the receiver. SNR percentiles are given with RQT data on the lower right.

The various graphs show parameter effects as a function of signal power for each of the UWB permutations. The reader is referred to Table 4.1.1 for Gaussian noise power level settings for each receiver. Also the power of all gated signals is expressed as the average power during the on-time of the gated cycle.

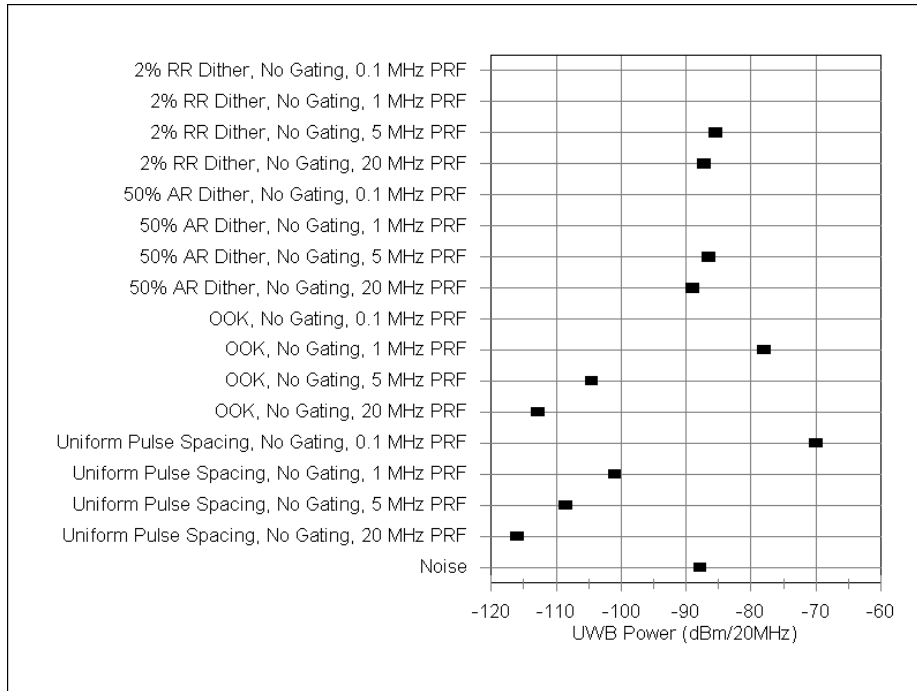


Figure 6.2.1. Non-gated UWB signal vs. signal power at BL (Rx 1).

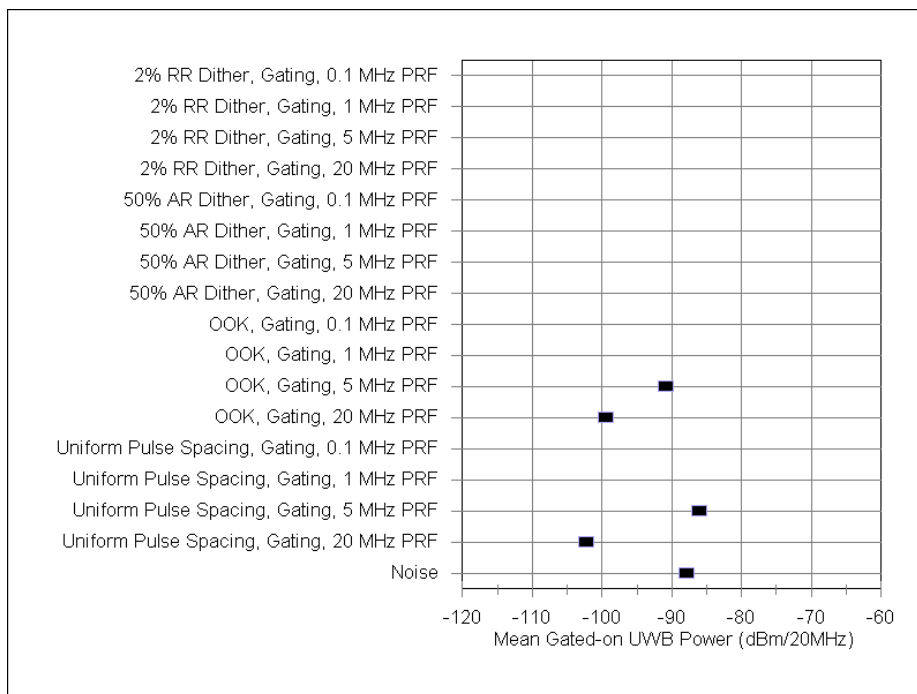


Figure 6.2.2. Gated UWB signal vs. signal power at BL (Rx 1).

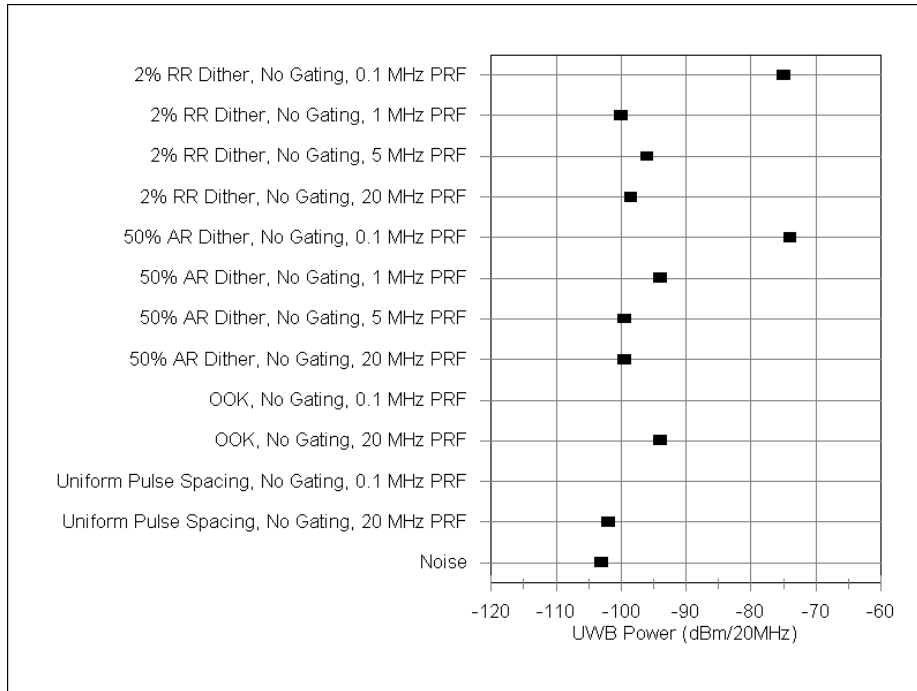


Figure 6.2.3. Non-gated UWB signal vs. signal power at BL (Rx 2).

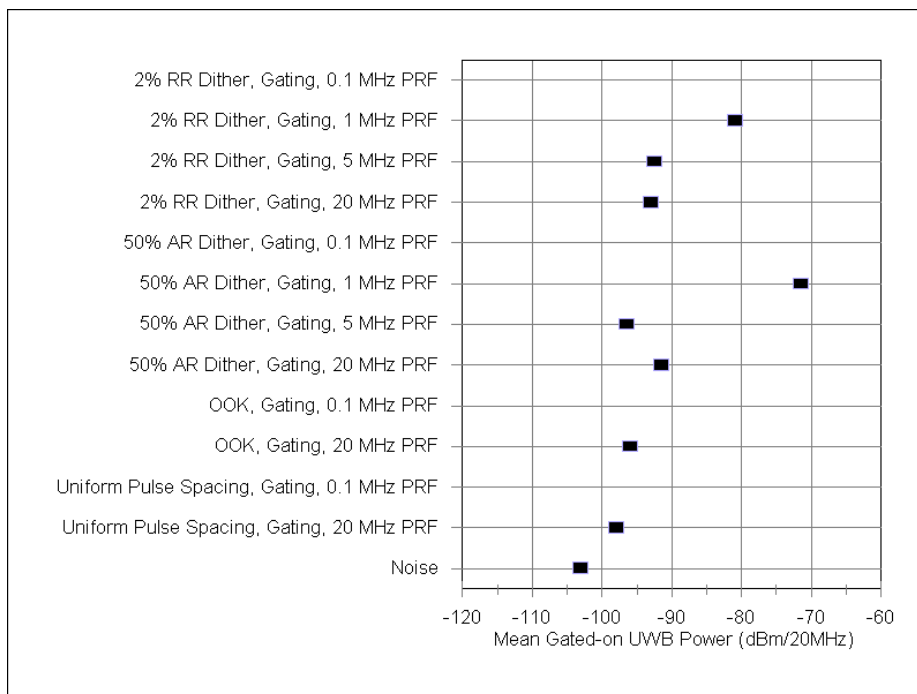


Figure 6.2.4. Gated UWB signal vs. signal power at BL (Rx 2).

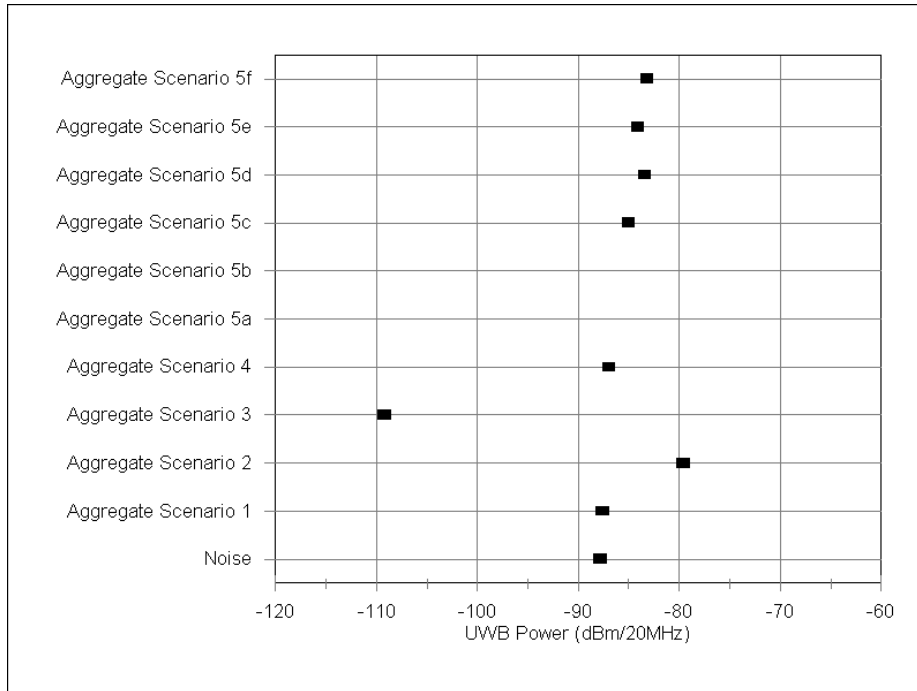


Figure 6.2.5. Aggregate UWB signal vs. signal power at BL (Rx 1).

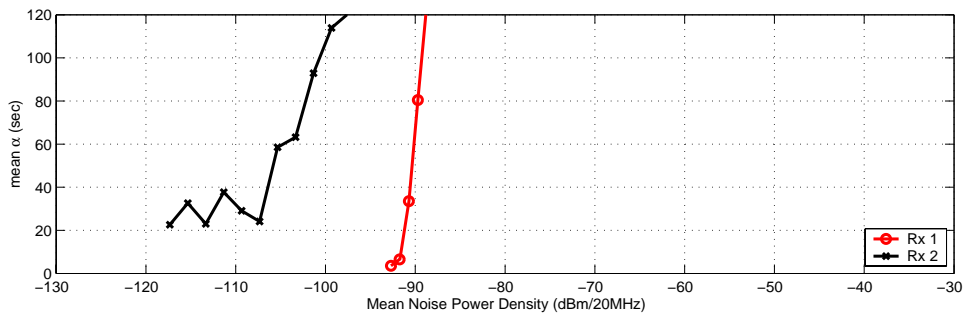


Figure 6.2.6. RQT of GPS receivers when exposed to Gaussian-noise interference.

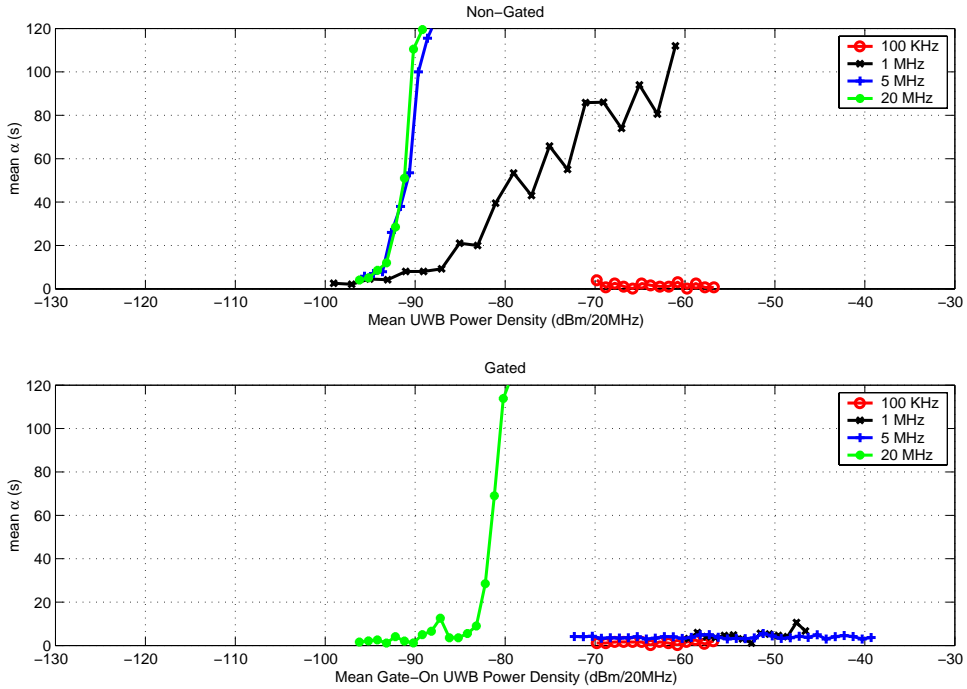


Figure 6.2.7. RQT of Rx 1 when exposed to 2%-RRD UWB interference.

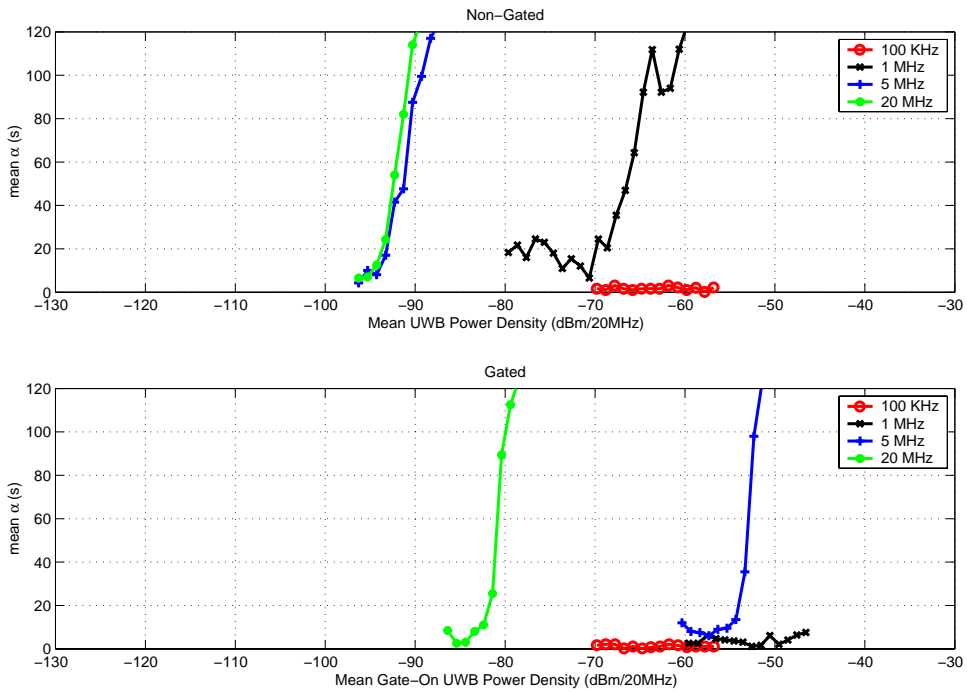


Figure 6.2.8. RQT of Rx 1 when exposed to 50%-ARD UWB interference.

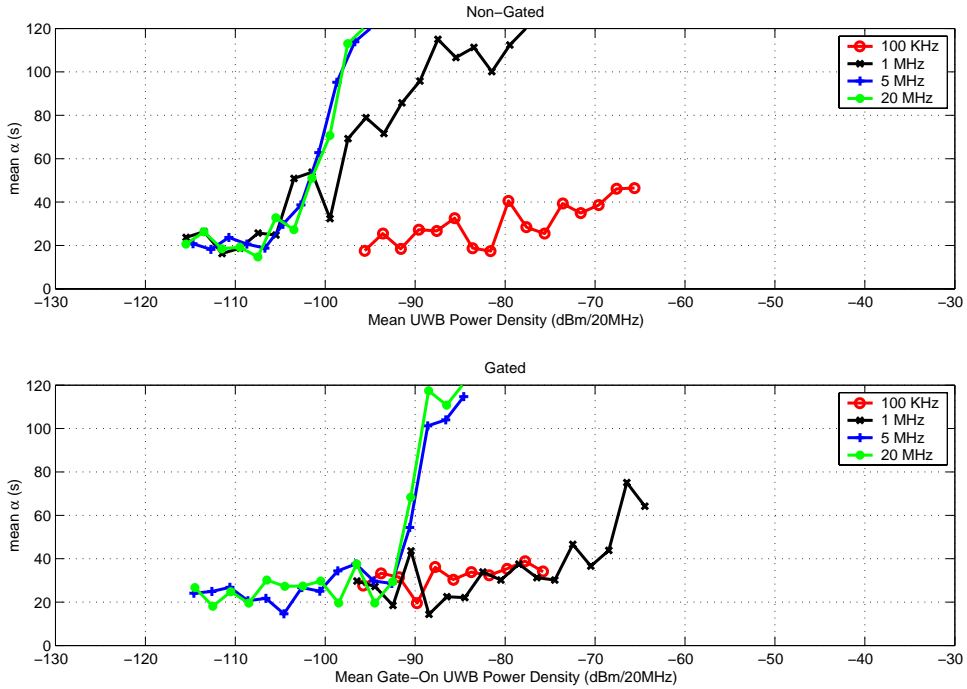


Figure 6.2.9. RQT of Rx 2 when exposed to 2%-RRD UWB interference.

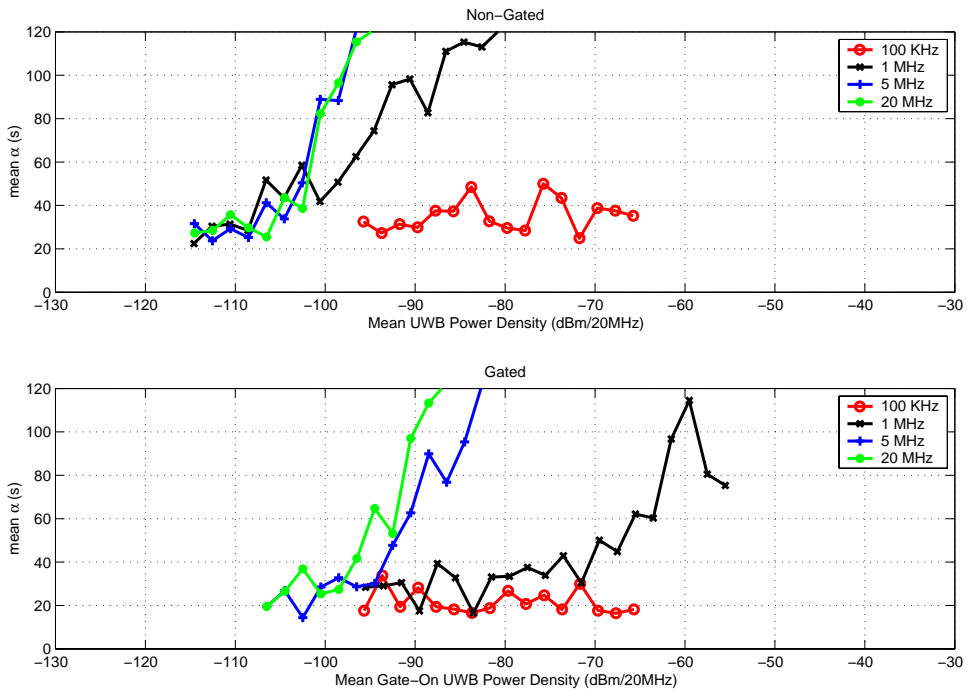


Figure 6.2.10. RQT of Rx 2 when exposed to 50%-ARD UWB interference.

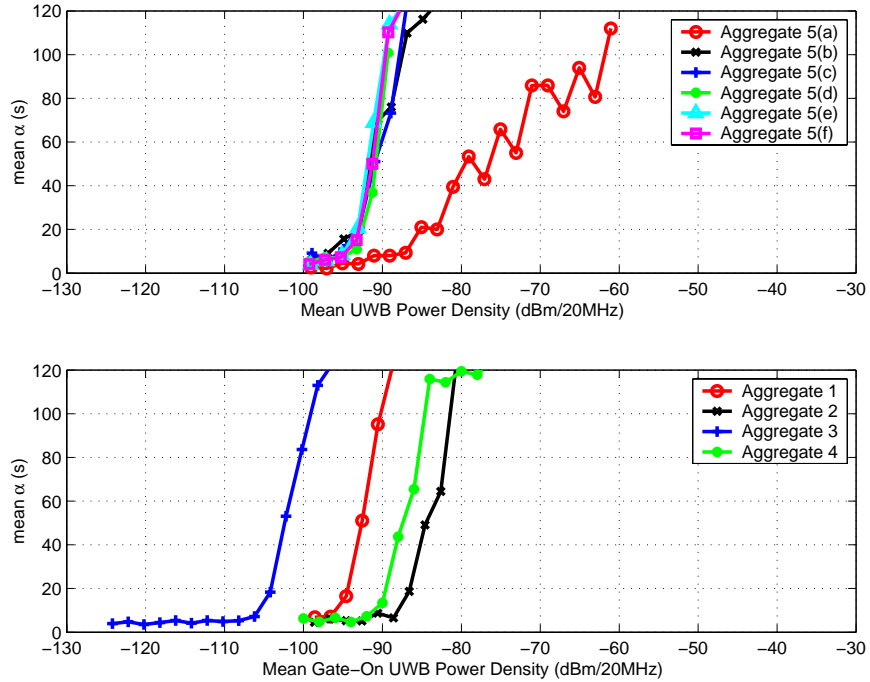


Figure 6.2.11. RQT of Rx 1 when exposed to aggregate UWB interference.

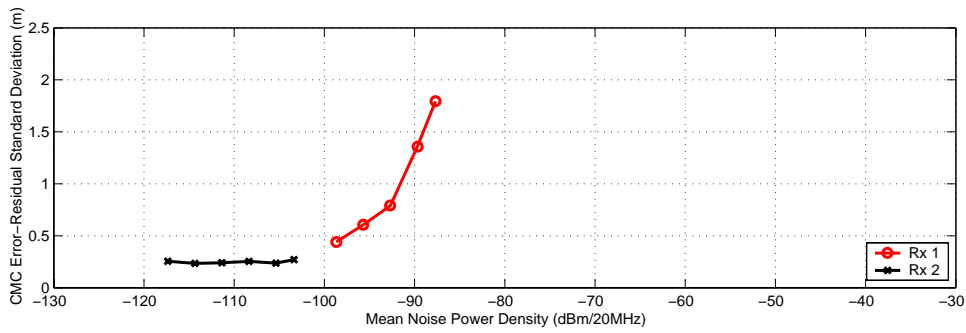


Figure 6.2.12. PSR accuracy of GPS receivers when exposed to Gaussian-noise interference.

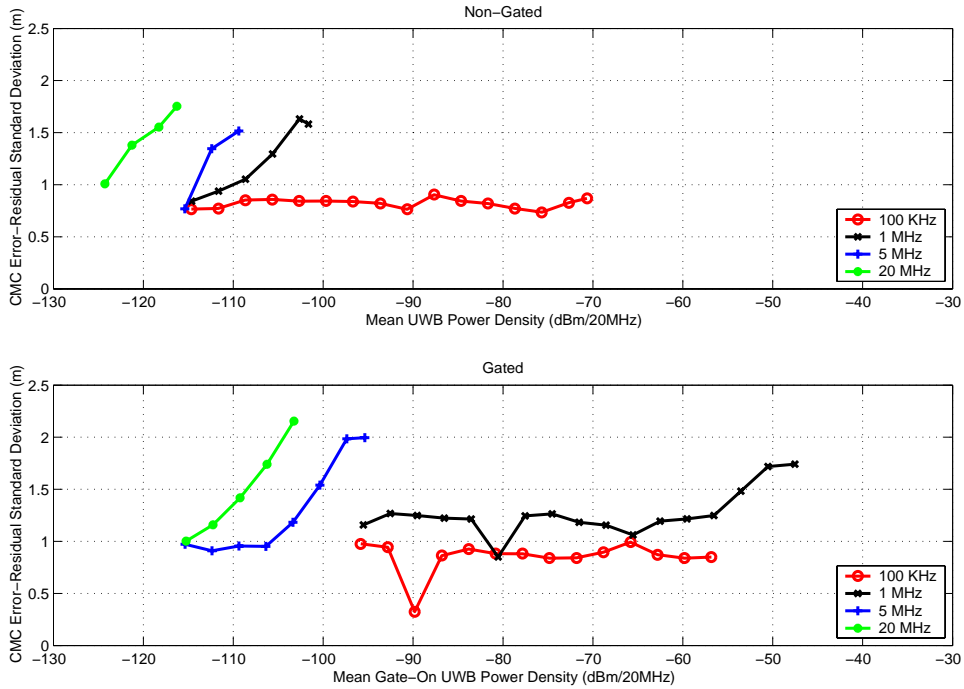


Figure 6.2.13. PSR accuracy of Rx 1 when exposed to UPS UWB interference.

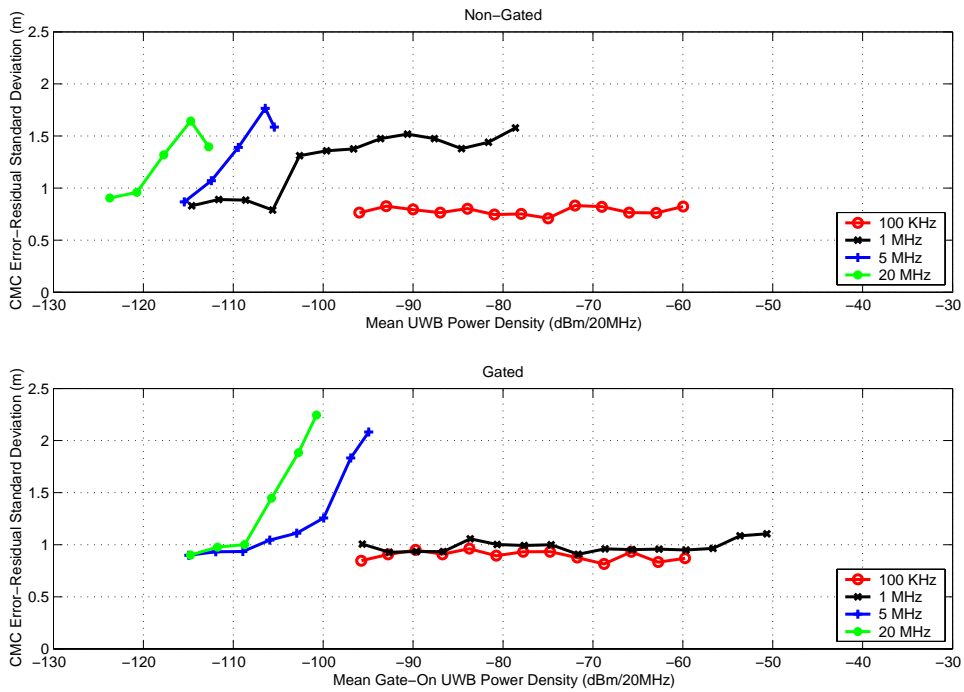


Figure 6.2.14. PSR accuracy of Rx 1 when exposed to OOK UWB interference.

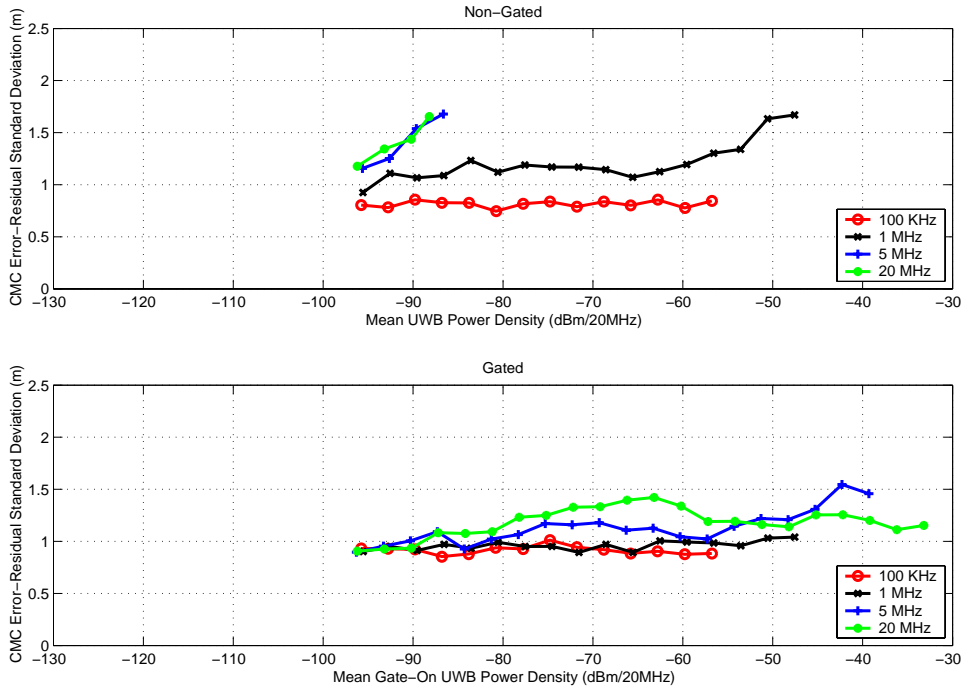


Figure 6.2.15. PSR accuracy of Rx 1 when exposed to 2%-RRD UWB interference.

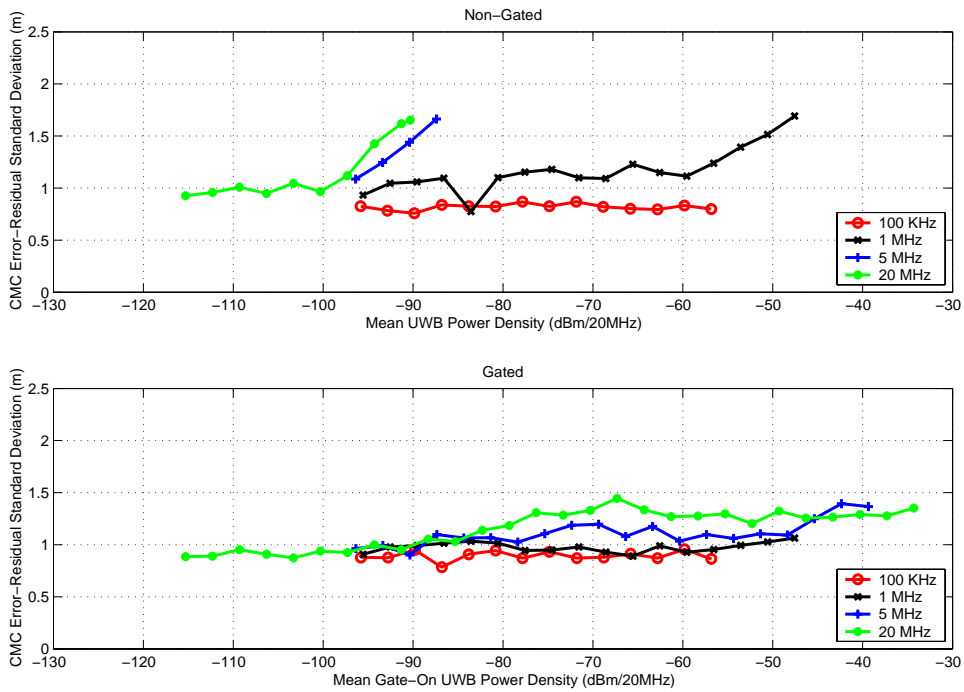


Figure 6.2.16. PSR accuracy of Rx 1 when exposed to 50%-ARD UWB interference.

6.3 Summary of Measurement Results

Because of the different receiver bandwidths and different signal processing techniques employed, each receiver responds in a different manner. In addition, there are certain trends in receiver response to UWB interference which can be identified and related to various characteristics of the UWB signals. In this section, these trends will be summarized for both receiver differences and variation in UWB signal interference.

6.3.1 Receiver Observations

Receiver 1 is a general purpose navigation receiver. Receiver 2 is a high-precision, semi-codeless receiver which relies heavily upon carrier phase information. It also has narrow correlator capabilities, and therefore wide bandwidths. It should be noted that Rx 2 was tested without the Gaussian-noise source, except for the Gaussian-noise interference test.

Several general observations can be made with respect to each receiver:

1. Figures 6.2.1 through 6.2.4 show that Rx 1 BL points occur at higher UWB signal powers for ARD and RRD, and Rx 2 showed BL at higher UWB signal powers for OOK and UPS.
2. As exemplified in Figure 6.2.6 and throughout the RQT results (e.g., Figures 6.2.7 through 6.2.10), the same RQT generally occurs at a higher interference power for Rx 1 than Rx 2.
3. Figures F.2.1 through F.2.33 show that Rx 1 is much more tolerant of cycle-slip conditions.
4. For most of the lower PRF cases (1-MHz and 0.1-MHz PRF), Rx 1 reported no change in C/N_0 despite the fact that UWB interference power was as much as 50 dB above the added Gaussian noise. This was also seen for Rx 2 for all UWB signal power levels and types.
5. Sometimes the receivers were able to reacquire at UWB signal power levels greater than the BL point (see Figures F.1.36, F.2.1, F.2.10 through F.2.15, F.2.18, F.2.19, F.2.21, F.2.22). This occurred more frequently with Rx 2.

From these and other observations, several conclusions can be drawn:

6. Because of its intended application, BL occurred for Rx 2 whenever there are cycle slips.
7. BL results show that Rx 2 is more tolerant of interference with spectral lines.
8. Reacquisition can sometimes occur at UWB power levels greater than the BL point for two reasons. One reason is that the BL point is probabilistic and can occur over a range of power levels from one time to the next. The other reason is that BL measurement duration is long, while maximum RQT is relatively short.
9. For Rx 1, the observational results are correlated to BL and RQT. For many of the UWB signals, CMC, ADR, cycles slips, and C/N_0 show significant changes and parallel RQT as the UWB interference power levels approached the BL point. However, for Rx 2 only RQT showed change prior to the BL point.

4. RQT has been found to be the most sensitive parameter for identifying interference effects on the receiver. In fact, sometimes RQT is elevated when UWB power levels are as much as 10 to 20 dB below the BL point (see Figures F.1.19, F.1.20, F.1.22, F.1.27, F.1.30, F.1.38, F.1.39, and F.2.20).

6.3.2 Variations Due to UWB Signal Characteristics

Aside from receiver differences, there are trends in receiver response related to the characteristics of the UWB signals themselves, such as pulse spacing, PRF, gating, and the accumulation of multiple UWB signals.

Pulse Spacing

Receiver effects can be directly related to the different modes of pulse spacing – UPS, dithering, and OOK. Any time the UWB signal has a uniform pulse spacing, there are spectral lines, and when these spectral lines lie within the GPS band, there is potential for alignment with spectral lines of the GPS signal. This alignment is particularly invasive as evidenced by BL at low UWB powers in Figures 6.2.1 and 6.2.2. Particularly for higher PRFs, where more power is gathered up into each of the spectral lines, Rx 1 breaks lock at power levels as much as 25 dB below the added noise. The same trends can be seen for CMC and ADR error-residual, and cycle slips.

On-off-keying, since it too has spectral lines, can have a significant impact on GPS receivers. This is evident in Figures 6.2.1, and 6.2.2, where for higher PRFs the BL point occurs by as much as 20 dB below the added noise. However, the effects of OOK are less detrimental than for UPS; this is because the spectral power is distributed between spectral lines and a noise component (see Appendix D). Also, as evidenced by comparing UPS with OOK in the APDs, OOK has the effect of increasing the peak-to-average noise power and decreasing the percentage of time the signal is present above the system noise, thus decreasing the impact on receiver performance.

Dithering reduces the impact of UWB interference on GPS receivers. As discussed in Section 4.1.2, dithering can reduce or eliminate spectral lines – thus spreading the power over the band and reducing the effects of interference. As evidenced by APDs such as those shown in Figures C.3.10 and C.3.12, UWB signals at high PRF rates (e.g., 5 and 20 MHz) are distributed similarly to Gaussian noise when limited to a 3-MHz bandwidth. This is in keeping with the BL results shown in Figures 6.2.1 through 6.2.4, where for higher PRFs, dithering shows BL results similar to Gaussian noise. For the lower PRFs of 1.0 and 0.1 MHz, the impact from dithered UWB signals is even further reduced.

Pulse Repetition Frequency

Higher PRFs have a greater detrimental effect for two reasons. One is that for those cases with spectral lines, greater power is gathered into each spectral line. The other reason is that higher PRFs result in a reduced peak to average power ratio and a greater percentage of time for which the signal is present. This is evident in measured APDs such as those shown in Figure C.3.9. For each of the plots in Figures 6.2.1 through 6.2.4, one can see a natural progression of the point of BL moving to lower UWB power densities as the PRF increases, irrespective of the pulse spacing mode. The same trends can be seen for RQT, CMC and ADR error-residual, and cycle slips.

Gating

Gating reduces the impact on receivers for two reasons. One is that, as mentioned in Section 4.1.2, the power of individual spectral lines is spread out into multiple lines, thus reducing the power contained in any single line. The other reason is that, for signals of equal gated-on power density, the percentage of time the signal is present is less with gating. For each of the parameters measured, one can readily see that for the same power density during the gated-on time, the detrimental effects are significantly reduced as compared to non-gated signals.

Accumulation of Multiple UWB Signals

With the aggregate of multiple asynchronous UWB signals, one would expect the sum of the signals to become more Gaussian noise-like in its distribution and effects on GPS receivers. There are several trends which can be noted when examining the characteristics of each of the aggregate scenarios described in Table 4.1.2.2. As shown in Figures C.3.30 and C.3.31, increasing the number of summed signals in scenario 5 causes the aggregate signal to become more Gaussian – the extent being dependent upon the bandwidth. Scenarios 2 and 4 are somewhat more impulsive in nature because of asynchronous gating applied to several of the signals. Scenarios 1 and 3 both have relatively Gaussian distributions; however, scenarios 3 and 4 both have strong spectral lines – scenario 3 being potentially more invasive, in that it has more power gathered up into lines spaced 10 MHz apart.

The characteristics of these aggregate signals can be directly related to the impact on receiver performance. As noted in Figure 6.2.5, scenarios 1 and 4 show BL test results similar to noise. Scenario 2, which is essentially the same as scenario 1 but with gating applied, shows a BL point at a lower gated-on power than its non-gated counterpart. Scenario 3 shows a BL point at a low signal power because, while its APD is Gaussian distributed, it has strong spectral lines (see Figure 6.3.2.1). Scenario 5 (*a* through *f*) shows effects similar to Gaussian noise for an aggregate of anything more than 2 signals.

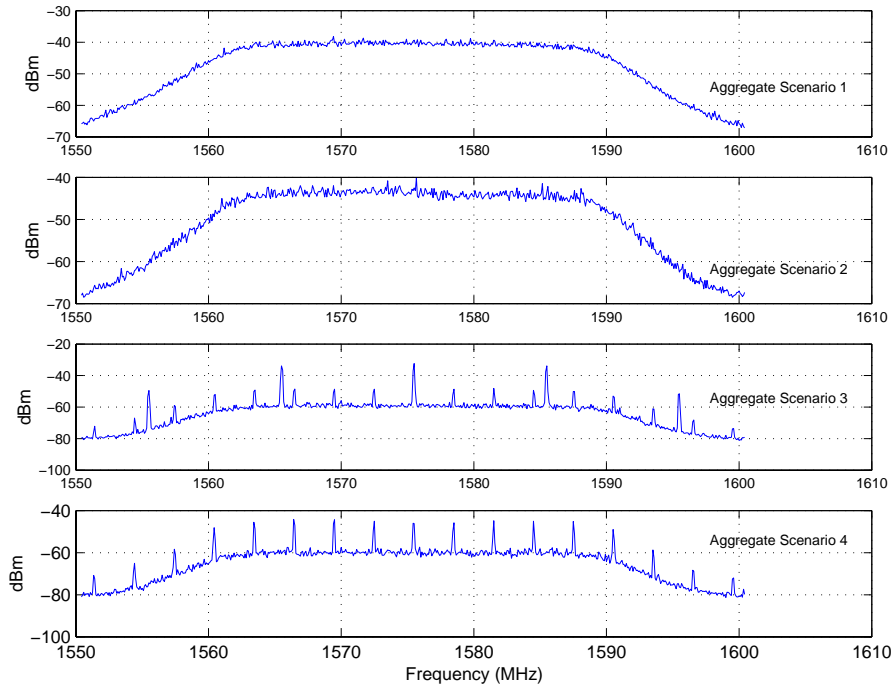


Figure 6.3.2.1. Spectral characteristics (through a 24-MHz filter) for aggregate case 1 through 4.

This Page Intentionally Left Blank

This Page Intentionally Left Blank